An Optical Frequency Transfer Link with the Remote Site Compensation

Qi Zang (臧琦)[1,3], Xiang Zhang(张翔) [1,3]*, Xue Deng (邓雪)[4], Qian Zhou (周茜)[1,2,3], Dan Wang (王丹)[1,2,3], Yucan Zhang (张钰灿)[1,2,3], Jing Gao (高静)[1,3], Dongdong Jiao (焦东东)[1,3], Guanjun Xu (许冠军)[1,2,3], Tao Liu (刘涛)[1,2,3,], Ruifang Dong (董瑞芳)[1,2,3***], Shougang Zhang(张首刚) [1,2,3]**

1 National Time Service Centre, Chinese Academy of Sciences, Xi'an 710600, China
2 University of Chinese Academy of Sciences, Beijing, 100039, China
3 Key Laboratory of Time Reference and Applications, Chinese Academy of Sciences, Xi'an, 710600, China
4 School of Communications and Information Engineering and School of Artificial Intelligence, Xi'an University of Posts and Telecommunications, Xi'an, 710121, China
**Corresponding author: zhangxiang@ntsc.ac.cn;*
***Corresponding author: taoliu@ntsc.ac.cn;*
****Corresponding author: dongruifang@ntsc.ac.cn*

In this paper, we present a remote time-base free technique for a coherent optical frequency transfer system via fiber. At the remote site, the thermal noise of the optical components is corrected along with the link phase noise caused by environmental effects. In this system, a 1 × 2 AOM is applied at the remote site, with the 1st light being used to eliminate the noise of the remote time base and interface with remote users while the 0th light is used to establish an active noise canceling loop. With this technique, a 10 MHz commercial oscillator, used as a time base at the remote site doesn't contribute to the noise of the transferred signal. An experimental system is constructed using a 150 km fiber spool to validate the proposed technique. After compensation, the overlapping Allan deviation of the transfer link is 7.42×10^{-15} at 1 s integration time and scales down to 1.07×10^{-18} at 10,000 s integration time. The uncertainty of the transmitted optical frequency is on the order of a few 10^{-19}. This significantly reduces the time-base requirements and costs for multi-user applications without compromising transfer accuracy. Meanwhile, these results show great potential for transferring ultra-stable optical frequency signals to remote sites, especially for point-to-multi-users.
PACS: 42.62.Eh;42.82.Bq;42.55.Wd;62.25.Fg;

1. Introduction

Optical atomic clocks have been developed rapidly in recent years[1-4]. The distribution of these high-precision clock reference signals is significant and has many important applications, such as geodesy, fundamental physics, timekeeping, global navigation, and astronomy[5-9].

Optical fiber links offer an ideal solution for users to coherently transfer stable optical frequency signals to remote sites, particularly for long-distance transmission and multi-users access to high-performance time and frequency signals[10-16]. Currently, remote ultra-stable laser comparison has been realized through optical frequency transmission via the field fiber link with 2,220 kilometers length by M. Schioppo *et al.* in 2022[17].

Unfortunately, the environmental temperature variations, vibration, and mechanical perturbations along the fiber links will dominate the fluctuations of transfer delay of the fiber links and introduce additional phase noise to the optical frequency signal. To overcome this problem, a local site active noise compensation technique was demonstrated by Ma *et al.* for the first time in 1994, which generally obtained the phase error from a beat note signal of round-trip and reference light to feed a servo system[18]. Based on this local phase noise cancellation scheme, various noise compensation links have been demonstrated by several research groups and have achieved remarkable results with point-to-point structures[19-24]. A point-to-multi-point access structure via the fiber topology model at local site compensation was demonstrated by Gesine Grosche in 2014[25]. After that, more flexible solutions using the branching method for optical frequency transfer with remote site compensation have been proposed[26-29]. In these schemes, the error signal is obtained by beating the single trip light against the third trip light in the fiber link, and the phase noise is compensated at the remote site. So, the remote time base has an influence on the precision of the transferred signal. In contrast, Ref [28] and [29] have achieved time-base-free optical frequency distribution at the remote site, avoiding the time-base noise accumulation with the growth of users. In their system, to eliminate the influence of time-base, an AOM is equipped out of the transfer loop at the remote site while its thermal noise and the additional mismatch of optical fiber cannot be compensated,

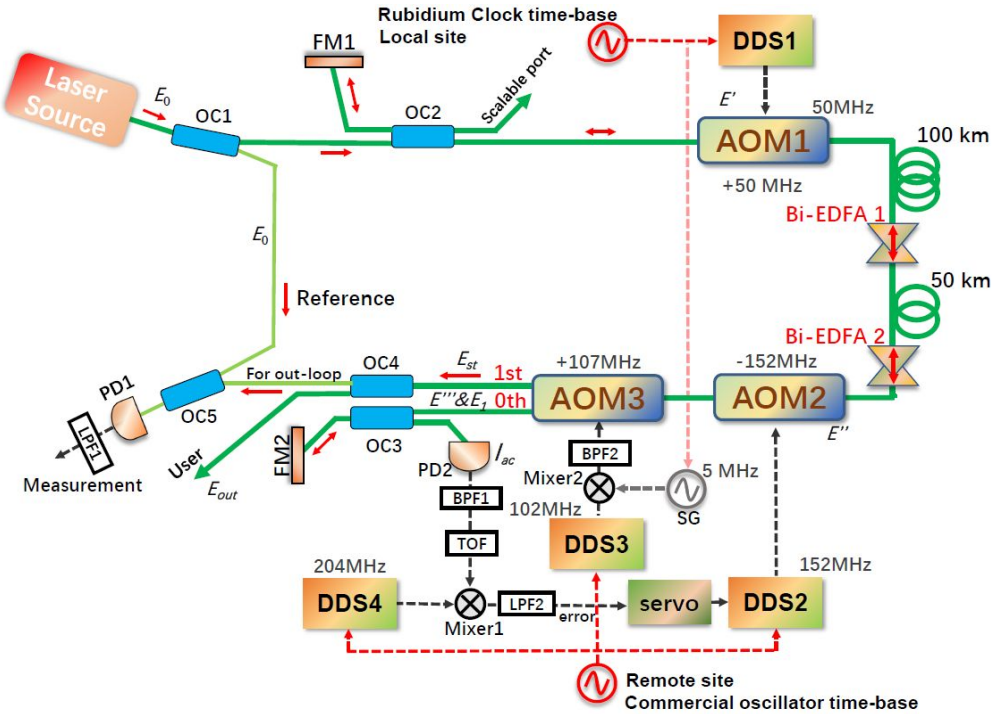

Figure.1 Diagram of the remote site compensation experimental setup; OC, optical coupler; FM, Faraday mirror; AOM, acousto-optic modulator; Bi-EDFA, bidirectional erbium-doped fiber amplifier; DDS, direct digital synthesizer; PD, photo-detector; Mixer, frequency mixer; BPF, band-pass filter; LPF, low-pass filter; TOF, tracking oscillator filter; SG, signal generator.

which will affect the transmission performance in an unstable external environment. Otherwise, Xue *et al.* demonstrated a novel remote site passive compensation technique for transferring the optical frequency through a branching fiber link. In their experiment, a high transmission instability was achieved to 3.7×10^{-19} at 10,000 s integration time with the same time-base[27]. In addition, the noise floor and transfer performance are effectively optimized by precise temperature control (~10 mK) of the transfer system at local and remote sites. However, the temperature control will increase the cost and complexity of the system. Hence, the most effective and simplest method is to design a remote site compensation-based optical frequency transfer system with a 10 MHz time-base free and temperature-insensitive structure by properly designing the fiber optics system.

In this paper, we demonstrate a novel time-base free optical frequency transfer method via a 150 km fiber link with remote site compensation. In our experiment, we utilize special choosing RF frequencies and a commercial 10 MHz oscillator to realize time base independence at the remote site. By optimizing the optical path design and inserting the phase compensation device into the compensation loop, the sensitivity of the transmission system to temperature changes can be further reduced, and the transmission performance can be improved. The induced phase noise of the fiber and the thermal noise of the optical devices are compensated by the active noise cancellation technique. By comparing the transferred optical frequency signal against the reference light, the 150 km fiber link relative instability is 7.42×10^{-15} at 1 s integration time and scales down to 1.07×10^{-18} at 10,000 s integration time as the $1/\tau$ slope. Meanwhile, the frequency uncertainty is a few 10^{-19} in this link. Otherwise, this scheme has an optimized mismatch of the interferometer and a better noise floor without temperature control in the system, showcasing its potential for ultra-stable optical frequency signal transfer among point-to-point or point-to-multi users. The paper is organized as follows. First, we illustrate the principle of time-base free at remote site compensation. Then, the experimental setup and the results are demonstrated including the instability in the time domain, the phase noise in the frequency domain, and the frequency transfer accuracy. Finally, the results are analyzed.

2. Principle

In this remote compensation scheme, the laser source is a commercial narrow-linewidth fiber laser (Koheras Basik E15) operating at 1550.12 nm with a linewidth of 0.1 kHz. Fig.1 shows the diagram of the experimental setup for optical frequency signal transfer through the fiber link. The initial electric field E_0 of the light from the laser can be expressed as (1)

$$E_0 = A_0 cos(\omega_0 t + \phi_0) \tag{1}$$

where A_0 is the amplitude, ω_0 is the angular frequency, and ϕ_0 is the phase of this transfer light. Then, the light passes through a 1×2 fiber optical coupler 1 (OC1) and a 2×2 OC2 to acousto-optic modulator 1 (AOM1). Here, the light is firstly frequency-shifted +50 MHz and the AOM1 driving frequency is from direct digital synthesizer 1 (DDS1), which is synchronized with the local rubidium clock time-base. Then the electric field becomes

$$E' = A'cos[(\omega_0 + \omega_{AOM1})t + \phi_0 + \phi_{AOM1}] \quad (2)$$

$\omega_{AOM1} = 2\pi \times 50$ MHz and ϕ_{AOM1} are the driving angular frequency and phase of AOM1. Then, the transferred light is coupled into the fiber link with a power of ~5 mW. For compensating fiber link loss (~0.2 dB/km), two bidirectional erbium-doped fiber amplifiers (Bi-EDFAs) are installed in the link.

When the fiber link output light arrives at the remote site, it is firstly frequency shifted by -152 MHz through AOM2, in which the electric field E'' of the -1st diffracted signal is

$$E'' = A''cos[(\omega_0 + \omega_{AOM1} - \omega_{AOM2})t + \phi_0 + \phi_{AOM1} - \phi_{AOM2} + \phi_{fiber}] \quad (3)$$

At this time, the noise from the fiber link ϕ_{fiber} and the effects of AOM2 are added to the transmitted light. AOM3 is a specially designed device, and the 1×2 structure has two output arms, that the 0th arm directly passes the light without frequency shift, while the 1st arm light is driven by DDS3 with a frequency of +102 MHz. Here, the 0th arm light and two Faraday mirrors (FM) form an active phase-locked loop with the 1×2 OC3. Assuming the fiber link phase noise in forward and backward directions is equal to the disturbance from the environment, the electric fields of the single trip and the third trip are expressed as (4) and (5):

$$E''' = A'''cos[(\omega_0 + \omega_{AOM1} - \omega_{AOM2})t + \phi_0 + \phi_{AOM1} - \phi_{AOM2} + \phi_{fiber} + \phi_{AOM3}^{0th}] \quad (4)$$

$$E_1 = A_1cos[(\omega_0 + 3\omega_{AOM1} - 3\omega_{AOM2})t + \phi_0 + 3\phi_{AOM1} - 3\phi_{AOM2} + 3\phi_{fiber} + 3\phi_{AOM3}^{0th}] \quad (5)$$

Photodetector 2 (PD2) extracts the phase noise by beat notes E''' and E_1. Consequently, this term of PD2, which carries twice the phase noise given by (6), and the beat note frequency is 204 MHz. Within the feedback bandwidth, the fiber-induced phase noise can be eliminated.

$$I_{ac} \propto 2A'''A_1cos[(2\omega_{AOM1} - 2\omega_{AOM2})t + 2\phi_{AOM1} - 2\phi_{AOM2} + 2\phi_{fiber} + 2\phi_{AOM3}^{0th}] \quad (6)$$

DDS4 generates another 204 MHz RF signal whose electric field is $E_{DDS4} = A_{DDS4}(\omega_{DDS4}t + \phi_{DDS4})$. Then the signal is mixed with I_{ac} and the error signals are flitted to the servo system. The servo system makes $\omega_{AOM1} - \omega_{AOM2} = \omega_{DDS4}$ and $\phi_{AOM1} - \phi_{AOM2} + \phi_{fiber} + \phi_{AOM3}^{0th} = \phi_{DDS4}$ achieves the link phase noise compensation.

When the transfer link is compensated, the single trip light of the remote site at the AOM3 1st arm is (7)

$$E_{st} = A_3cos[(\omega_0 - \omega_{DDS4} + \omega_{AOM3}^{1th})t + \phi_0 - \phi_{DDS4} + \phi_{AOM3}^{1th}] \quad (7)$$

Notice, here the ω_{AOM3}^{1th} and ϕ_{AOM3}^{1th} depends on remote time-base, so make $\omega_{AOM3}^{1th} = \omega_{DDS4}$ and $\phi_{AOM3}^{1th} = \phi_{DDS4}$. Consequently, the $E_{out} = E_{st}$ is

$$E_{out} = A_{out}cos[(\omega_0)t + \phi_0] \quad (8)$$

We can see that E_{out} is not affected by the local or remote time base from (8).

3. Experimental Setup and Results

We have shown the diagram of the experimental configuration in Fig.1. The transfer link is 150 km and consists of two fiber spools: one span is 100 km, another span is 50 km, and the single trip loss is more than 30 dB. Two Bi-EDFAs with a gain of 16 dB are placed at the link to compensate for the fiber loss. To achieve a heterodyned beat note signal at PD1, we up mix the drive frequency of AOM3 to 107 MHz by mixer 2 with a signal generator (RS SMB100A) that locks on the local rubidium clock. With this configuration, we obtain a 5 MHz beat note signal by combining the AOM3 1st arm light and the local laser reference light with the 1×2 OC5. Because of the complex RF signals in the system, a DC-5 MHz low-pass filter (LPF) 1 is applied after PD1 and a 100-110 MHz band-pass filter (BPF) 2 before the SMA interface of AOM3. Meanwhile, a tracking oscillator filter (TOF) is equipped after the PD2 to amplify and stabilize the signal amplitude with a center frequency of 204 MHz. Mixer 1 down mixes the DDS4 signal and the in-loop signal to obtain an error for the servo system. Here, these two signals are both divided by 204 to 1 MHz with two programmable digital frequency dividers. To guarantee that the system is working properly, a DC-100 kHz LPF2 is applied after the mixer. In addition, the drive amplitude

should be taken into account and carefully adjusted to the 0th and 1st diffracted light powers of the AOM3.

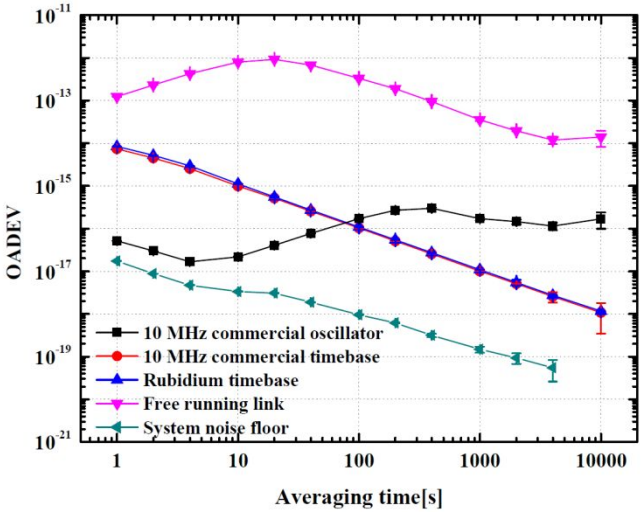

Figure.2 The overlapping ADEV of the 150 km fiber transfer link at remote site compensation. The pink triangle curve is the free-running link. The red dot and blue triangle curves are compensated link of 10 MHz commercial time-base and rubidium clock time-base, respectively. The black square curve is the commercial 10 MHz. And the green triangle curve is the system noise floor.

To measure the performance of the compensation link, we use a no-dead-time frequency counter (FXE K+K) with the Π -type mode and a gate time of 1 s to record the out-loop data and calculate the Overlapping Allan Deviation (OADEV) in the time domain. The results as shown in Fig.2, the relative frequency instability of the light after the compensated fiber link with the rubidium clock time-base is 8.43×10^{-15} at 1 s integration time, decreases and reaches 1.16×10^{-18} at 10,000 s integration time (blue triangle curve) with the $1/\tau$ slope. The red dot curve illustrates the OADEV result of the 10 MHz commercial time-base in which the 1 s integration time is 7.42×10^{-15} and scales down to 1.07×10^{-18} at 10,000 s integration time, also as the $1/\tau$ slope. From these two instability results, it becomes evident that when the transfer link is compensated, the remote site time-base doesn't affects the transfer precision, as the transfer results are very similar and not affected by the time base. As a comparison, the black square curve illustrates the OADEV of a commercial 10 MHz oscillator as the remote time base. The pink triangle curve is the free-running link when the remote compensation system is off. In our experiment, it is observed that the stability of the optical frequency is improved by approximately 4 orders of magnitude at 10,000 s integration time by the remote site compensation system. The green triangle curve shows the noise floor of the 1 m transfer link by active phase noise cancellation. Here, we find that the noise floor reached the 10^{-20} level at 2,000 s integration time, which is more than two orders of magnitude in the short term (1 s) and one order of magnitude in the long term (4,000 s) lower than the compensation link in this system, while the OADEV slope is limited by the temperature variation-induced length fluctuation of the interferometer mismatch fiber in the measurement system.

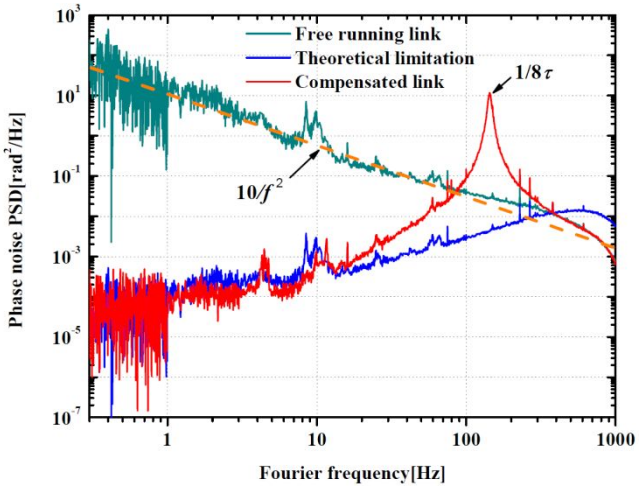

Figure.3 The phase noise PSDs of the 150 km fiber transfer link. The green curve is the free-running link. The red and blue curves are the compensated link and the theoretical limitation, respectively.

To analyze the phase noise of this link in the frequency domain, a phase noise analyzer (Rohde & Schwarz FSWP8) is utilized to measure the phase noise power spectral density (PSD) for both compensated and free-running configurations over the 150 km optical signal transfer, as depicted in Fig.3. When the link is free running, the green curve illustrates that the phase noise PSD $S_{fiber}(f)$ agrees with formula (9)[22] type below 200 Hz as the yellow dashed line, mainly limited by the flicker phase noise.

$$S_{fiber}(f) = h_0 / f^2 \tag{9}$$

where f is the Fourier frequency, h_0 is dependent on environmental disturbances of fiber links, and equals 10 in this 150 km transfer system. Once the compensation system is engaged in the remote site by the users, the relative phase noise is effectively canceled down by approximately 50 dB at 1 Hz, shown as the red curve. The compensated phase noise PSD is close to 10^{-4} rad²/Hz in the low-frequency range of between 0.5 Hz to 10 Hz, which means that the compensated fiber link is mainly constrained by the white phase noise after stabilizing the transfer link. Meanwhile, according to the results of the red curve, it can be seen that the feedback bandwidth of the system is about 167 Hz $(1/8\tau)$[29]. The theoretical phase noise $S_{theoretical}(f)$ limitation from free-running is calculated by (10)[22, 29]

$$S_{theoretical}(f)=\frac{1}{3}(2\pi f\tau)^2 S_{fiber}(f) \qquad (10)$$

and plotted as the blue curve in Fig.3, and it has a good agreement with the compensated link.

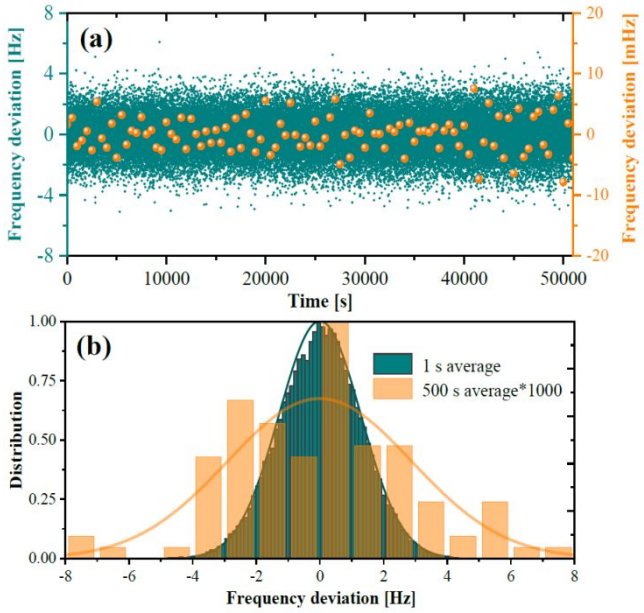

Figure.4 (a) The frequency deviation of the 150 km fiber transfer link. The frequency data were recorded by the frequency counter with 1 s gate time (green points, left axis). We calculated unweighted mean (Π -type) values for all cycle-slip free 500 s long segments, resulting in 51,000 data points (orange dots, right axis, enlarged scale). (b) Histograms (green bars) and Gaussian fits (green curves) for frequency values as taken with Π -type frequency counters with 1 s gate time, and orange bars and curves for 103 phase-coherent 500-second frequency averages.

For further evaluation of this compensation system, we also evaluate the accuracy of optical frequency transfer. Fig.4(a) shows the frequency deviations of the recorded data by the FXE K+K counter with a 1 s gate time and Π -type mode. The data are measured over successive 51,000 s (green point, left axis). We can obtain 103 points by averaging the data every 500 seconds, as shown in Fig.4(a) (orange points, right axis). Histograms and Gaussian fits of the frequency deviation are also shown in Fig.4(b). To better show the details of the distribution, the frequency deviation axis has been enlarged by 1000 times. According to the Gaussian fit in Fig.4(b), the calculated results demonstrate that the mean frequency is shifted by -7.9 μ Hz (-4.1 $\times 10^{-20}$), and the standard deviation of the 500 s data points is 2.90 mHz (1.5 $\times 10^{-17}$), which is more than two orders of magnitude smaller than the OADEV at 1 s as expected for this Π -type evaluation.

4. Conclusion

In conclusion, we demonstrate a remote time-base-free technique for a 150 km coherence optical frequency transfer link, and the fiber-induced optical phase noise is compensated at the remote site. In this scheme, an ultra-stable optical frequency reference can be reproduced using a commercial 10 MHz oscillator as the time-base instead of a high-performance clock by the remote user. In addition, to optimize the impact of the asymmetric part of the fiber on the performance of the system, we use a 1 $\times$2 AOM in the loop that the 0th light is used to build a servo loop and the 1st diffracted light is launched to users. Based on this experimental setup, the OADEV of the relative optical frequency transfer instability is 7.42$\times 10^{-15}$ at 1 s integration time and decreases as the $1/\tau$ slope to 1.07 $\times 10^{-18}$ at 10,000 s integration time. Benefiting from the time-base firee technique, the noise floor at 1 s and 10,000 s are improved by almost two and one order of magnitude, respectively. The frequency uncertainty of the light after transferring through the fiber is a few 10^{-19}. With this phase noise compensation setup, once the system is locked, the phase noise can be effectively suppressed by approximately 50 dB at 1 Hz. The results demonstrate significant potential for constructing a flexible, convenient, and cost-effective point-to-point or point-to-multi-users topology structure in this setup. This alternative method of optical frequency transfer complements existing local or remote site compensation systems and is compatible with cascade transfer links.

Funding

This work was supported by The Strategic Priority Research Program of the Chinese Academy of Sciences (Grant No. XDB21000000); The Open Project Fund of State Key Laboratory of Transient Optics and Photonics, Chinese Academy of Sciences (Grant No. SKLST202011); National Natural Science Foundation of China (Grant No. 12103059); National Natural Science Foundation of China (Grant No. 12103059, 12303076 and 12303077) and Planned project of Xi'an Bureau of science and technology, China (Grant No. E019XK104).

References

[1] Bloom B J, Nicholson T L, Williams J R, Campbell S L, Bishof M, Zhang X, Zhang W, Bromley S L, Ye J. An optical lattice clock with accuracy and stability at the 10(-18) level [J]. Nature, 2014, 506(7486): 71-5.

[2] Huntemann N, Sanner C, Lipphardt B, Tamm C, Peik E. Single-Ion Atomic Clock with 3×10-18 Systematic Uncertainty [J]. Physical Review Letters, 2016, 116(6): 063001.

[3] Beloy K, Bodine M I, Bothwell T, Brewer S M, Zhang X. Frequency ratio measurements at 18-

digit accuracy using an optical clock network [J]. Nature, 591(7851): 564-9.
[4] Oelker, Hutson, R B, Kennedy, C J, Sonderhouse, Bothwell, Goban, Kedar, Sanner. Demonstration of 4.8 x10(-17) stability at 1s for two independent optical clocks [J].
[5] Grotti J, Koller S, Vogt S, Hfner S, Sterr U, Lisdat C, Denker H, Voigt C, Timmen L, Rolland A. Geodesy and metrology with a transportable optical clock [J]. Nature Physics, 2018,
[6] Lisdat C, Grosche G, Quintin N, Shi C, Raupach S, Grebing C, Nicolodi D, Stefani F, Al-Masoudi A, D ?Rscher S. A clock network for geodesy and fundamental science [J]. Nature Communications, 2016, 7(
[7] Droste S, Grebing C, Leute J, Holzwarth R. Characterization of a 450-km Baseline GPS Carrier-Phase Link using an Optical Fiber Link, F, 2014 [C].
[8] Cliche J F, Shillue B. Applications of control Precision timing control for radioastronomy maintaining femtosecond synchronization in the atacama large millimeter array [J]. IEEE Control Systems Magazine, 2006, 26(1): 19-26.
[9] Riehle, Fritz. Towards a Re-definition of the Second Based on Optical Atomic Clocks [J]. Comptes Rendus Physique, 2015, 16(5): 506-15.
[10] Riehle, Fritz. Optical clock networks [J]. Nature Photonics, 2017, 11(1): 25-31.
[11] Predehl K, Grosche G, Raupach S, Droste S, Terra O, Alnis J, Legero T, Haensch T W, Udem T, Holzwarth R. A 920-Kilometer Optical Fiber Link for Frequency Metrology at the 19th Decimal Place [J]. Science, 2012, 336(6080): 441.
[12] Kim J, Schnatz H, Wu D S, Marra G, Richardson D J, Slavík R. Optical injection locking-based amplification in phase-coherent transfer of optical frequencies [J]. Optics Letters, 2015,
[13] Calonico D, Bertacco E K, Calosso C E, Clivati C, Costanzo G A, Frittelli M, Godone A, Mura A, Poli N, Sutyrin D V. High-accuracy coherent optical frequency transfer over a doubled 642-km fiber link [J]. Applied Physics B, 2014, 117(3): 979-86.
[14] Chiodo N, Quintin N, Stefani F, Wiotte F, Camisard E, Chardonnet C, Santarelli G, Amy-Klein A, Pottie P E, Lopez O. Cascaded optical fiber link using the Internet network for remote clocks comparison [J]. Optics Express, 2015, 23(26): 33927.
[15] Droste S, Ozimek F, Udem T, Predehl K, Holzwarth R. Optical-frequency transfer over a single-span 1840 km fiber link [J]. Physical Review Letters, 2014, 111(11): 110801.
[16] Qi Z, Honglei Q, Kan Z, Xiang Z, Wenxiang X, Faxi C, Wenyu Z, Tao L, Ruifang D, Shougang Z. High-precision Time-Frequency Signal Simultaneous Transfer System via a WDM-based Fiber Link [J]. 2021,
[17] Schioppo M, Kronjger J, Silva A, Ilieva R, Paterson J, B Ay Nham C, Bowden W, Hill I, Hobson R, Vianello A. Comparing ultrastable lasers at 7 × 1017 fractional frequency instability through a 2220 km optical fibre network [J]. Nature Communications,
[18] Ma L S, Jungner P, Ye J, Hall J L. Delivering the same optical frequency at two places: accurate cancellation of phase noise introduced by an optical fiber or other time-varying path [J]. Optics Letters, 1994, 19(21): 1777-9.
[19] Deng, Zang, Jiao, Dongdong, Jing, Zhang, Xiang, Wang, Dong, Ruifang. Coherent phase transfer via fiber using heterodyne optical phase locking as optical amplification [J]. APPLIED OPTICS, 2018, 57(32): 9620–4.
[20] S, M, F, Raupach, A, Koczwara, G, Grosche. Optical frequency transfer via a 660 km underground fiber link using a remote Brillouin amplifier [J]. Optics Express, 2014,
[21] Lopez O, Haboucha A, Chanteau B, Chardonnet C, Amy-Klein A, Santarelli G. Ultra-stable long distance optical frequency distribution using the Internet fiber network [J]. Optics express, 2012, 20(21): 23518-26.
[22] Newbury N R, Williams P A, Swann W C. Coherent transfer of an optical carrier over 251 km [J]. Optics Letters, 2007, 32(21): 3056.
[23] Williams P A, Swann W C, Newbury N R. High-stability transfer of an optical frequency over long fiber-optic links [J]. Journal of the Optical Society of America B, 2008, 25(1284-93.
[24] Zang Q, Deng X, Zhang X, Wang D, Zhou Q, Jiao D, Xu G, Gao J, Liu J, Liu T. Cascaded transfer of optical frequency with a relay station over a 224 km deployed fiber link [J]. Infrared physics and technology, 2023,
[25] Grosche, Gesine. Eavesdropping time and frequency: phase noise cancellation along a time-varying path, such as an optical fiber [J]. Optics Letters, 2014, 39(9): 2545.
[26] Schediwy S W, Gozzard D, Baldwin K, Orr B J, Warrington R B, Aben G, Luiten A N. High-precision optical-frequency dissemination on branching optical-fiber networks [J]. Optics Letters, 2013, 38(15): 2893-6.
[27] Xue R, Hu L, Shen J, Chen J, Wu G. Branching optical frequency transfer with enhanced post automatic phase noise cancellation [J]. Journal of Lightwave Technology, 2021, 39(14): 4638-45.
[28] Wu L, Jiang Y, Ma C, Yu H, Ma L. Coherence transfer of subhertz-linewidth laser light via an optical fiber noise compensated by remote users [J]. Optics Letters, 2016, 41(18): 4368.

[29] Ma Chaoqun, Wu Lifei, Gu Jiao, Chen Yanhe, Chen Guoqing. Delay Effect on Coherent Transfer of Optical Frequency Based on a Triple-Pass Scheme [J]. CHINESE PHYSICS LETTERS, 2018, 35(8): 5.